Carbohydrate Polymers 104 (2014) 59–65

Contents lists available at ScienceDirect

Carbohydrate Polymers

journal homepage: www.elsevier.com/locate/carbpol

All-cellulose nanocomposite film made from bagasse cellulose nanofibers for food packaging application

Moein Ghaderi [a,*], Mohammad Mousavi [a], Hossein Yousefi [b], Mohsen Labbafi [a]

[a] Bioprocess Engineering Laboratory (BPEL), Department of Food Science, Engineering & Technology, Faculty of Agricultural Engineering and Technology, University of Tehran, P.O. Box 4111, Karaj 31587-77871, Iran
[b] Department of Wood Engineering and Technology, Gorgan University of Agricultural Sciences and Natural Resources, Gorgan 4913815739, Iran

ARTICLE INFO

Article history:
Received 9 November 2013
Received in revised form
17 December 2013
Accepted 5 January 2014
Available online 10 January 2014

Keywords:
All-cellulose nanocomposite
Food packaging
Bagasse

ABSTRACT

All-cellulose nanocomposite (ACNC) film was produced from sugarcane bagasse nanofibers using N,N-dimethylacetamide/lithium chloride solvent. The average diameter of bagasse fibers (14 μm) was downsized to 39 nm after disk grinding process. X-ray diffraction showed that apparent crystallinity and crystallite size decreased relatively to an increased duration of dissolution time. Thermogravimetric analysis confirmed that thermal stability of the ACNC was slightly less than that of the pure cellulose nanofiber sheet. Tensile strength of the fiber sheet, nanofiber sheet and ACNC prepared with 10 min dissolution time were 8, 101 and 140 MPa, respectively. Water vapor permeability (WVP) of the ACNC film increased relatively to an increased duration of dissolution time. ACNC can be considered as a multi-performance material with potential for application in cellulose-based food packaging owing to its promising properties (tough, bio-based, biodegradable and acceptable levels of WVP).

1. Introduction

Nowadays, most materials used in the packaging industry are produced from fossil fuels (Shchipunov, 2012). Materials made from fossil fuels are non-biodegradable in structure so widespread use of such materials presents a serious cause for concern in terms of their impact on the environment (Tang, Kumar, Alavi, & Sandeep, 2012). This consideration has prompted much research in recent years into the development of products such as bio-based polymers that could replace this non-biodegradable packaging in the food industry. Many bio-based polymers such as cellulose, starch, chitin and chitosan have been studied for application in packaging, and cellulose has been identified as a suitable material (Ray & Bousmina, 2005; Tang et al., 2012).

Cellulose is the most abundant biopolymer in existence and it is derived from readily available biomass (Kimura et al., 1999). Cellulose is a homopolysaccharide, composed of (β-1,4)-linked-glucopyranose units (Abraham et al., 2011) and nanostructures. In recent years cellulose nanostructures have attracted much research attention and are used in many industrial applications (Gibson, Lee, Ko, & Reneker, 2007; Mazalevska, Struszczyk, Chrzanowski, & Krucińska, 2011). The importance of cellulose nanostructure can be attributed to its inherent properties such as biodegradability and renewability (Chen et al., 2011) high specific strength and stiffness (Zimmermann, Bordeanu, & Strub, 2010; Afra, Yousefi, Hadilam, & Nishino, 2013), high reinforcing potential and large specific surface area (Abraham et al., 2011). There is a wide variety of wood and non-wood resources suitable for the production of cellulose nanostructures. The use of non-wood resources such as agricultural residue is interestingly now on the rise due to shortages of natural resources such as wood as well as concerns over the environmental impact of other widely used materials (Villar, Revilla Gómez, Carbajo, & Simón, 2009; Alila et al., 2012). For example, sugarcane bagasse, which is used as the raw material in this current study, is a low value agricultural residue. 1.6 billion tons of sugarcane (in 2011) is produced annually in the world (Chandel, da Silva, Carvalho, & Singh, 2012) and 1 ton of sugarcane generates 280 kg of bagasse (Cerqueira & Meireles, 2007). Bagasse contains a considerable amount of cellulose (40–50%) (Sun, Sun, Zhao, & Sun, 2004), but the greater part of bagasse remains unused.

All-cellulose nanocomposites are classified as biocomposite, a class of materials that has been recognized and studied during the past decade (Nishino, Matsuda, & Hirao, 2004). The matrix and reinforcement phases in these biocomposite materials are non-crystalline and undissolved cellulose, respectively (Soykeabkaew, Sian, Geo, Nishino, & Peijs, 2009; Yousefi, Faezipour, Nishino, Shakeri, & Ebrahimi, 2011a,b). These nanocomposites have promising properties, for example they are a completely bio-based material and as such fully biodegradable; they also have remarkably high mechanical performance and transparency (Nishino et al.,

* Corresponding author. Tel.: +98 26 3224 8804; fax: +98 26 3224 9453.
E-mail address: moein.ghaderi87@gmail.com (M. Ghaderi).

0144-8617/$ – see front matter © 2014 Elsevier Ltd. All rights reserved.
http://dx.doi.org/10.1016/j.carbpol.2014.01.013

2004; Gindl & Keckes, 2005; Duchemin, Mathew, & Oksman, 2009; Yousefi et al., 2010; Yousefi et al., 2011a,b). These characteristics give composite materials the potential for many applications (Nishino et al., 2004; Gindl & Keckes, 2005; Soykeabkaew, Arimoto, Nishino, & Peijs, 2008). Thus, the objective of this work was to produce all-cellulose nanocomposite from bagasse nanofiber and to investigate properties of the nanocomposite in terms of its suitability for food packaging.

2. Materials and methods

2.1. Materials and chemicals

Sugarcane bagasse was obtained from plantations in Khuzestan, Iran. Dimethyl acetamide (DMAc) (C_4H_9NO) was purchased from Scharlau Co., Spain. Acetone ($(CH_3)_2CO$), ethanol (CH_3CH_2OH), sodium hydroxide, potassium hydroxide, LiCl, sodium chlorite ($NaClO_2$) and anthraquinone ($C_{14}H_8O_2$) were supplied from Merck Chemical Co. (Darmstadt, Germany).

2.2. Preparation of cellulose fibers and nanofiber

The dried bagasse was first de-pithed by screening and then cooked in a digester with a solution of sodium hydroxide (20 wt.%) and anthraquinone (0.1 wt.%) at 170 °C for 1.5 h (dried bagasse to liquor ratio of 1:6). The yield of this pulping process was 60%. The digested bagasse was then washed with distilled water to remove lignin and hemicellulose. The bleaching process involved three steps with sodium chlorite at pH 4 (adjusted by acetic acid). The elimination of residual hemicellulose was also performed with potassium hydroxide aqueous solution (10 wt.%) at 80 °C for 2 h. Alpha-cellulose content was measured according to the TAPPI T 203 cm-99 standard.

The water slurry containing 1 wt.% sugarcane bagasse fiber was passed twice through a disk grinder (Masuko Co., Japan) at 1500 rpm. The well-stirred sugarcane suspension (0.5 wt.%) of bagasse nanofiber was filtered by vacuuming to make nanofiber sheets and then dried in a hot press (100 °C and 2 MPa for 1 h). These sheets of nanofiber, with the thickness range of 50 to 70 μm, were used as the starting material for the production of all-cellulose nanocomposite (ACNC).

2.3. ACNC production

The nanofiber sheets, as prepared in the previously described stage, were activated by immersion in distilled water, acetone and dimethyl acetamide for 2 h at ambient temperature successively. The nanofiber sheets were then submerged in a solution of DMAc/LiCl (8% LiCl) for six durations of dissolution time, ranging from 5 to 120 min at room temperature (DMAc and LiCl were first oven-dried at 105 °C to avoid any negative effect of water on the dissolution of cellulose). Samples were then submerged in ethanol for 16 h at ambient temperature during which the ethanol was replaced 10 times to rinse the solvent. The rinsed sheets were then dried by a hot press (at 2 MPa at 78 °C for 1 h) to prepare ACNC. The thickness of ACNC was 60–90 μm depending on the immersing time. Hereafter, the various ACNC samples will be denoted in relation to the duration of dissolution time; for example, the one prepared with a dissolution time of 5 min is termed ACNC-5.

2.4. Measurements

2.4.1. X-ray diffraction

X-ray diffraction tests were done using an X-ray diffractometer (INEL-Equinox-3000, France). Specimens were irradiated by Cu Kα radiation, created by an INEL-Equinox-3000 at 40 kV, 30 mA, in a perpendicular direction to the sample surface. For qualitative analysis, XRD patterns were recorded in the interval $10^\circ \leq 2\theta \leq 40^\circ$. Step size which was used was 0.03°.

Crystallinity index (CrI) evaluations were calculated by the following equation (Eq. (1)) (Segal, Creely, Martin, & Conrad, 1959):

$$\mathrm{CrI} = \left(\frac{I - I'}{I}\right) \times 100\% \quad (1)$$

where I is the diffraction intensity assigned to (2 0 0) plane of cellulose I_β. I' is the intensity measured at $2\theta = 18^\circ$, where the maximum happens in a diffractogram for the non-crystalline cellulose.

Crystallite size of the cellulose was assessed by Scherrer's equation (Eq. (2)) (Kakudo & Kasai, 1972):

$$D = \left(\frac{\lambda}{\beta \cos\theta}\right) \quad (2)$$

where D is the crystal size, λ is the X-ray wavelength (0.15418 nm), θ is the Bragg angle for the (2 0 0) reflection and β is the corrected integral width.

2.4.2. Field emission scanning electron microscope (FE-SEM)

Observation of the nanofiber sheets was made for fiber surface, cross section and broken surface and nanocomposites were observed by a field emission scanning electron microscope (FE-SEM) (Hitachi S-4160) operating at 10 kW. Specimen surfaces were coated with gold nanoparticles prior to observations.

2.4.3. Thermogravimetric analysis (TGA)

Thermal degradation behavior of cellulose nanofibers and nanocomposite was appraised using thermogravimetric analysis (TGA) (STA N-1500, Scinco Co., South Korea). The thermograms were run under a nitrogen atmosphere (to avoid premature degradation) at a heating rate of 10 °C/min using a high-resolution method over a temperature range of 30–600 °C.

2.4.4. Water vapor permeability (WVP)

Water vapor permeability (WVP) of the tested cellulose nanofiber and ACNC film was measured gravimetrically according to the modified ASTM E96-80 standard. The films were trimmed to a certain size and were then sealed to a glass dish (3 cm diameter), containing 100 g anhydrous calcium chloride (Merck, Germany) with relative humidity of around 0% RH. The dish was placed in a desiccator preserved at 75% RH with saturated sodium chloride (Merck, Germany). Water vapor was transmitted through the films and absorbed by the desiccant, evaluations were determined by measuring the weight gain. Mass changes were recorded, as the equilibration determination, at time zero and at every 6 h for four days. Calculations were made for flux, slope of the mathematical least squares regression of mass versus time (g/s), using Excel 2007 (Microsoft Co., USA) software. WVP was evaluated from the following equation (Eq. (3)) (Mauer, Smith, & Labuza, 2000):

$$\mathrm{WVP} = \left(\frac{\mathrm{Flux}}{AP_0(\mathrm{RH}_1 - \mathrm{RH}_2)}\right) \times x \quad (3)$$

where x is film thickness (m), A is the area of the film surface exposed to permeant (m^2), P_0 (1753.55 Pa at 25 °C) is the vapor pressure of pure water (Pa), and $(RH_1 - RH_2)$ is the relative humidity gradient used in the experiment.

2.4.5. Mechanical properties

Mechanical properties of specimens were measured using a tensile tester (M350-10CT, Testometric Co., Ltd., Rochdale, Lancashire, England) at room temperature. Gauge length was determined in the specimens at 20 mm and widths were 4 mm. Rates for load cell and extension rate were 1000 N and 1 mm min^{-1}, respectively. The average value and standard deviation of tensile strength, Young's

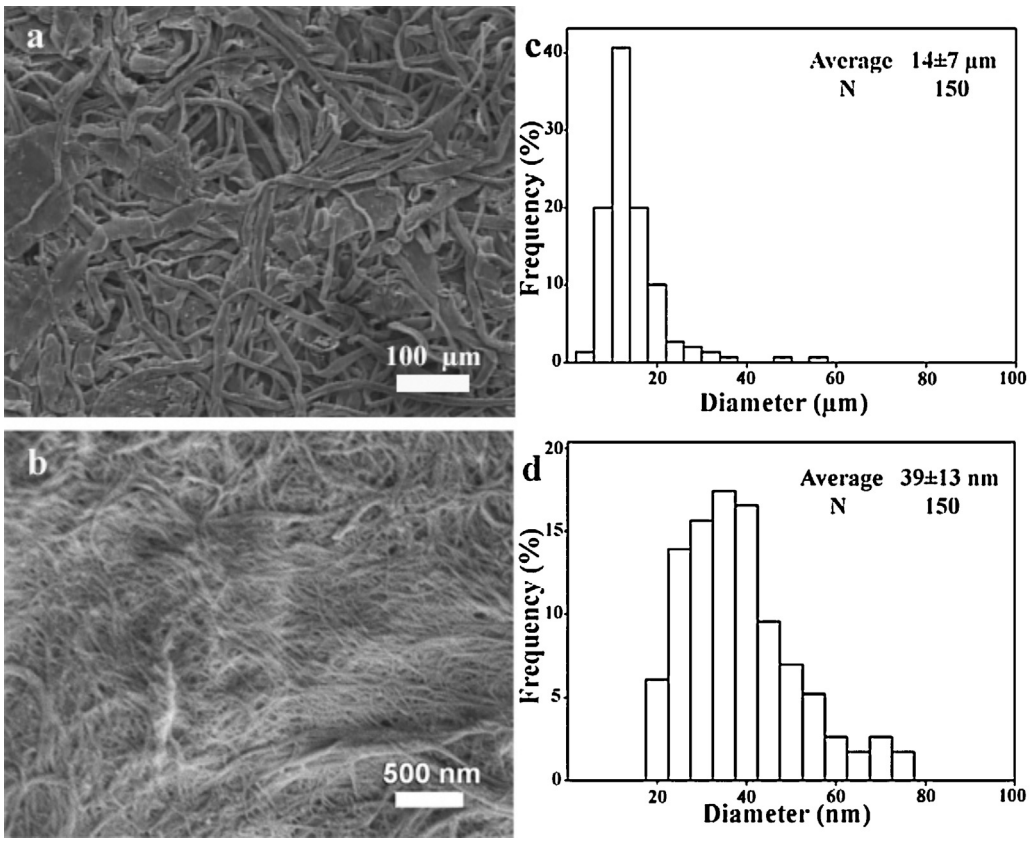

Fig. 1. FE-SEM micrographs of (a) the original fiber of sugarcane bagasse and (b) nanofibers produced by grinding. Diameter distribution of (c) fibers and (d) nanofibers. The average diameter and number of measured micro- and nanofibers are shown on Fig. 1c and d.

modulus (E), toughness and strain at break were evaluated for at least 5 of the tested specimens.

2.5. Statistical analysis

Statistical analysis was performed with SPSS 13 (SPSS Inc., Chicago, Illinois, USA) software. Tests for analysis of variance and means comparison (Duncan's Test) were applied with significance level of 0.05. The correlation analysis was determined by Pearson's test.

3. Results and discussion

3.1. Fiber and nanofiber sheets

After pulping and bleaching, the obtained alpha-cellulose content was 92 ± 2%, which shows that non-cellulosic impurities such as lignin and hemicellulose were almost removed and highly purified cellulose was produced.

Fig. 1 shows FE-SEM micrographs for (a) bleached bagasse fiber and (b) nanofiber produced by the disk grinding process. Diameter distributions of cellulose fiber and nanofiber produced by grinding are shown in Fig. 1c and d, respectively. As shown, the primary purified fibers of bagasse had a mean average diameter of about 14 μm. The shear and compression forces of the grinding process facilitated conversion of the primary purified bagasse fiber to cellulose nanofiber with an average diameter of 39 nm (about 360 times less than that of the unprocessed material). This extreme downsizing in dimension caused decreased roughness and pore size in the nanofiber sheets compared to the unprocessed sheets.

Fig. 2 shows the X-ray diffraction profile of the nanofiber sheet and ACNC. Peak intensity at $2\theta = 18^{\circ}$ increased according to an

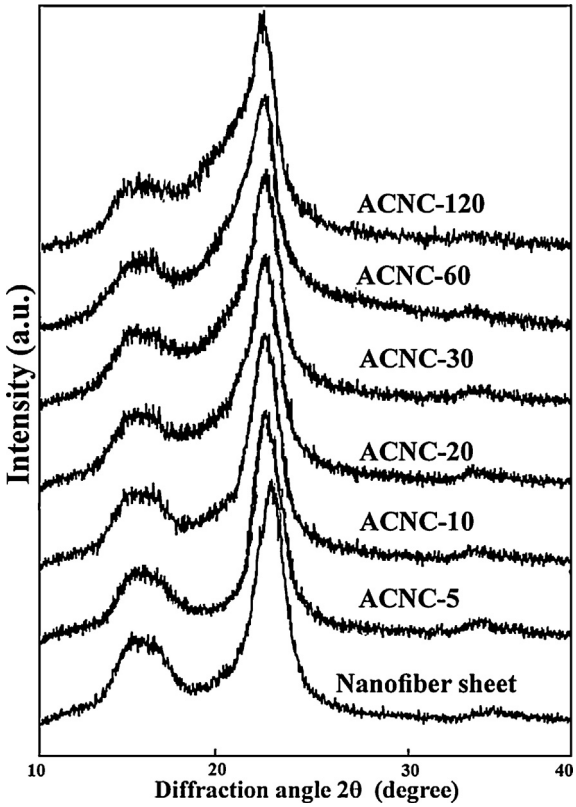

Fig. 2. X-ray diffraction profiles of nanofiber sheet and ACNC (taken by irradiating Cu Kα at 40 kV, 30 mA).

Table 1
Effect of grinding process and duration of dissolution time on the apparent crystallinity and crystallite size of fiber, nanofiber and ACNC.

Sample	Apparent crystallinity (%)	Crystallite size (nm)
Fiber	74.2	4.00
Nanofiber	72.9	3.70
ACNC-5	72.5	3.52
ACNC-10	72.3	3.40
ACNC-20	71.5	3.35
ACNC-30	70.1	3.30
ACNC-60	68.4	3.21
ACNC-120	65.0	3.10

increased duration of dissolution time, such that an increased duration of dissolution time produced a greater dissolution of the cellulose crystals, which resulted in an increased non-crystalline content (Han and Yan, 2010; Yousefi et al., 2011a).

Table 1 presents evaluations of specimens in terms of apparent crystallinity and crystallite size. Grinding process and the increase of dissolution time had both negative effect on apparent crystallinity and crystallite size. The outer chains of the crystallites became separated as a result of the shearing and compressive forces applied during the grinding process, thus reducing crystallinity and crystallite size. These forces caused cleavage of the crystallites and an increase in non-crystalline parts (Yousefi et al., 2010, 2011a). Fig. 2, shows that with increasing duration of dissolution time, the peak at $2\theta = 22.5^{\circ}$ was shifted to the left and it also became broader.

The effect of dissolution time induced a loss of crystallinity and reduced crystallite size; these effects can be attributed to the effect of more solvent penetrating the spaces between the crystallites and dissolved amorphous sections, as well as the outer chains of the crystallites (Nishino et al., 2004; Duchemin et al., 2009; Yousefi et al., 2010, 2011a).

Fig. 3 shows a thermogravimetric analysis' curves for the nanofiber sheet and ACNC. As shown, the thermal stability of ACNC decreased according to the partial dissolution process. This reduction in thermal stability can be attributed to diminution in apparent crystallinity due to an increased duration of partial dissolution time. Initial weight loss in the curves is related to the elimination of moisture and initial thermal decomposition. The onset degradation temperature of the cellulose nanofiber and ACNC-120 films were 176.9 and 174.1 °C, respectively. The lower onset temperature indicates a lower thermal stability for ACNC compared to that of the nanofiber sheet and this effect can be attributed to lower crystallinity of the ACNC as determined by results of the X-ray diffraction analysis (Swatloski, Spear, Holbrey, & Rogers, 2002).

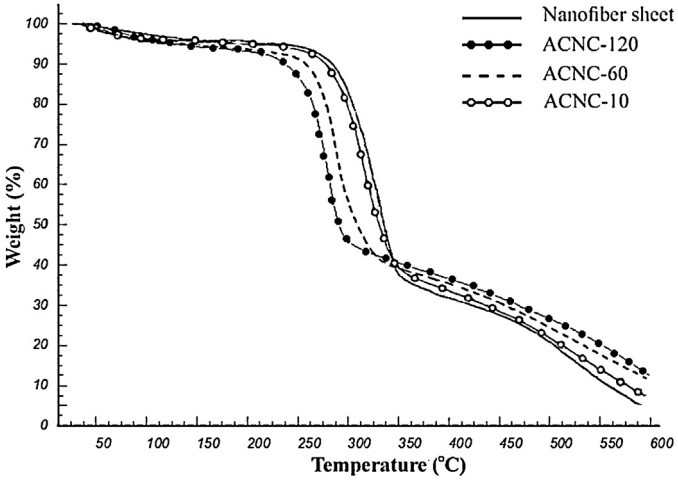

Fig. 3. Thermogravimetric analysis curves of nanofiber sheet and ACNC.

Table 2 shows the results of WVP of the cellulose nanofiber and ACNC sheets at different durations of partial dissolution. The WVP value of the cellulose nanofiber sheet was obtained at about

Table 2
Effect of dissolution time on the water vapor permeability, toughness and Young's modulus (E) of ACNCs prepared at different duration of dissolution times.

Film	Dissolution time (min)	WVP ($g\,m^{-1}\,s^{-1}\,Pa^{-1} \times 10^{-11}$)	E (GPa)	Toughness ($m\,N\,m^{-3}$)
Nanofiber sheet	0	2.46 ± 0.11^{d}	10.1 ± 0.5^{b}	2.31 ± 0.45^{d}
ACNC-5	5	2.7 ± 0.13^{d}	9.8 ± 0.3^{b}	6.21 ± 0.26^{c}
ACNC-10	10	5.2 ± 0.11^{c}	12.8 ± 0.4^{a}	8.07 ± 0.18^{b}
ACNC-20	20	5.46 ± 0.20^{c}	12.5 ± 0.3^{a}	8.97 ± 0.40^{ab}
ACNC-30	30	6.44 ± 0.47^{b}	12.2 ± 0.5^{a}	9.11 ± 0.35^{ab}
ACNC-60	60	6.48 ± 0.26^{b}	11.3 ± 0.4^{ab}	9.88 ± 0.24^{a}
ACNC-120	120	8.68 ± 0.34^{a}	8.2 ± 0.6^{c}	9.54 ± 0.50^{a}

$P < 0.05$

Table 3
Comparison of the water vapor permeability and tensile strength of nanofiber sheet and ACNC together with that of oil-derived synthetic and biodegradable films.

Sample	Tensile strength (MPa)[a]	WVP ($g\,m^{-1}\,s^{-1}\,Pa^{-1} \times 10^{-11}$)[a]	References
Nanofiber sheet	101	2.46	This work
ACNC-10	140	5.2	This work
Corn starch plasticized with glycerol	7.1	8.68	Piermaria, Pinotti, Garcia, & Abraham, 2009
Gellan gum plasticized with glycerol	30.0	20.8	Piermaria et al., 2009
Methyl cellulose	NR[b]	9.2	Park and Chinnan, 1995
Cellulose acetate/triethyl citrate/clay hybrid composites	105	NR	Park, Misra, Drzal, & Mohanty, 2004
Agar-based nanocomposite (10% clay)	36.87	150	Rhim, 2011
Cellophane	85.8	8.4	Shellhammer & Krochta, 1997
Sodium casein plasticized with glycerol	22.5	15.1	Piermaria et al., 2009
LDPE	13	0.036	Jiménez, Fabra, Talens, & Chiralt, 2012
HDPE	27.8	0.02	Smith, 1986
MFC (made from sugar beet)	104	NR	Leitner, Hinterstoisser, Wastyn, Keckes, & Gindl, 2007
NFC	180	NR	Svagan, Azizi Samir, & Berglund, 2007
ACNC	156	NR	Yousefi et al., 2010

[a] Data presented as mean.
[b] NR: not reported.

2.46×10^{-11} ($g\,m^{-1}\,s^{-1}\,Pa^{-1}$), and it shows a significant increase to 8.68×10^{-11} ($g\,m^{-1}\,s^{-1}\,Pa^{-1}$) under the dissolution duration of 120 min. Therefore, WVP evaluations increased according to longer duration of dissolution time. However, this increase in WVP was not significantly different compared to that of the nanofiber sheet over shorter durations of dissolution time. According to these conclusions, water vapor can transfer more easily through the matrix phase compared to rate of transfer in the reinforcement one, as the matrix phase possesses less order chains. Hence, WVP increased with an increased duration of dissolution time. In addition, with a longer duration of dissolution time, the ACNC sheet showed more shrinkage due to the effects of internal stresses; hence, ACNC increased in thickness, leading to warped films and separation of the cellulose nanofibers that created voids (Duchemin et al., 2009; Huber, Müssig, Curnow, Pang, Bickerton, & Staiger, 2012). Therefore, increased evaluations of WVP were recorded from processing with an increased duration of dissolution time.

Table 3 presents the WVP value of ACNC-10 compared to that of several biodegradable and non-biodegradable films. The ACNC sheet produced in this work possessed a lower WVP than that of protein film and carbohydrate films. Therefore, ACNC produced with shorter dissolution times had the capability to be replaced with the other biodegradable packaging materials.

Fig. 4 shows the effect of partial dissolution time on mechanical properties of ACNC. Fig. 4a shows stress–strain curves of the fiber and nanofiber sheets as well as evaluations for ACNC. As shown, tensile strength of the samples increased around twelve fold by converting bagasse fiber to nanofiber. This increase in tensile strength can be attributed to the following effects: (i) the production of smaller fibers makes tougher nanofiber sheets because it creates a tighter network with more junction points; (ii) the numbers of defect points of microfibers such as lumens and pits were omitted by downsizing fibers from micro- to nano-scales, resulting in a delayed breakup of the samples.

Fig. 4b shows the effect of dissolution time on tensile strength of ACNC. As shown, the tensile strength of ACNC increased under increased duration of dissolution time to 10 min and it reached 140 MPa. Tensile strength decreased under a dissolution time longer than 10 min. This increase in tensile strength can be attributed to the fact that at dissolution duration of over ten minutes, an adequate amount of non-crystalline cellulose was produced to weld the undissolved nanofiber cores during the pressing and drying procedures (Yousefi et al., 2011a,b). Over longer durations of dissolution time, tensile strength of the samples decreased because the ratio of the non-crystalline phase to undissolved parts increased, and that produced non-crystalline cellulose with weaker mechanical properties compared to the undissolved cellulose I_β played a main role in tensile strength. A decrease in the degree of polymerization at longer durations of dissolution time also had negative effect on tensile properties (Duchemin et al., 2009).

Table 2 shows the results of Young's modulus (E) of the cellulose nanofiber and ACNC sheets at different durations of partial dissolution. As the duration of dissolution time increased, the Young's modulus of ACNC increased significantly, reaching the highest value of E = 12.8 GPa at 10 min dissolution time and then dropped at the longer dissolution times. It seems the ratio of reinforcement and matrix phases reached optimum after 10 min dissolution time for cementing adjacent nanofibers. Table 2 shows also the results of toughness of the cellulose nanofiber and ACNC sheets at different durations of partial dissolution. As can be seen, the toughness of the samples with the increased duration of dissolution time followed an increasing trend.

Table 3 shows tensile strength evaluations for several biodegradable and non-biodegradable films. As can be seen, ten-

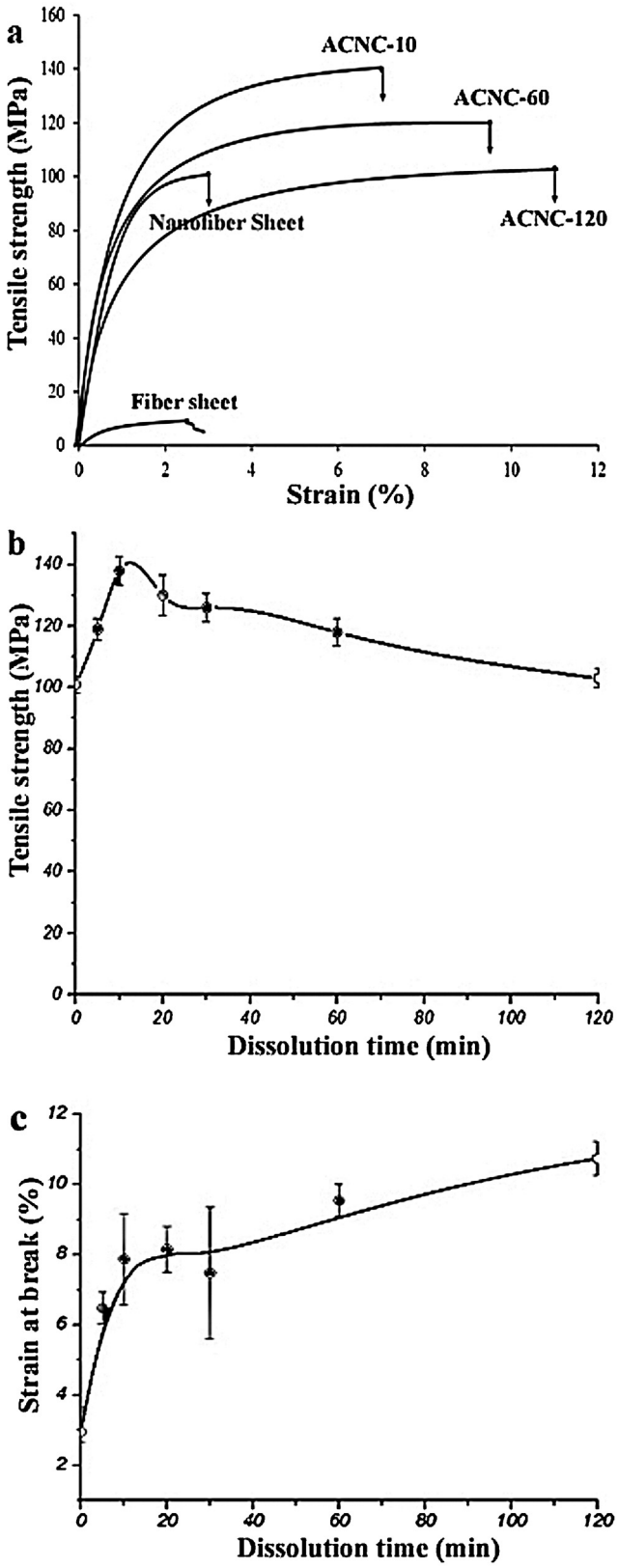

Fig. 4. Effect of dissolution time on the mechanical properties of ACNC. Stress–strain curves (a) of fiber sheet, nanofiber sheet and ACNC. (b) Tensile strength and (c) strain at break.

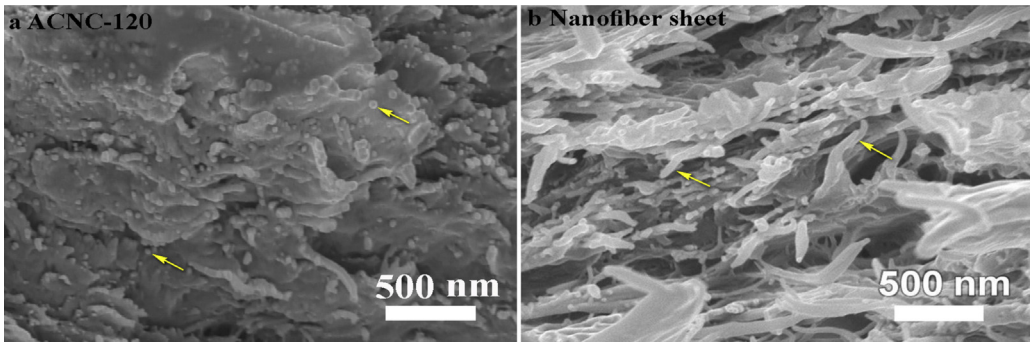

Fig. 5. FE-SEM micrographs of the tensile-broken surface of (a) ACNC–120 and (b) nanofiber sheet. Arrows show the pulled out nanofibers in Fig. 5b and broken nanofibers in Fig. 5a. Scale bars are 500 nm.

sile strength of the ACNC produced over 10 min was lesser or higher than that of the other biodegradable and non-biodegradable films.

Fig. 4c shows the effect of duration of dissolution time on strain at break evaluations of the ACNC. As can be observed, the strain at break of the samples with the increased duration of dissolution time followed an increasing trend. This increasing trend can be attributed to the fact that with increasing duration of dissolution time, the portion of non-crystalline cellulose increased, resulting in better chain entanglement and sliding, increasing strain at break. A highly negative correlation was found between crystallite size with strain at break ($r = -0.96$; $P < 0.01$) and apparent crystallinity with strain at break ($r = -0.88$; $P < 0.01$) values.

Fig. 5 shows the FE-SEM micrographs of evaluations for tensile-broken surface of (a) nanofiber sheet and (b) ACNC-120. In Fig. 5a, arrows show pulled-out nanofibers under tensile stress. In the case of ACNC (Fig. 5b), the nanofibers were broken under tensile stress. This is because the non-crystalline structure was able to make a strong welding between undissolved nanofiber core; hence, an effective interface/interphase could be created and a fully-consolidated structure was formed through which tensile stress was evenly distributed in the matrix-reinforcement network.

4. Conclusions

All-cellulose nanocomposite was satisfactorily produced by partial dissolution or surface selective method from nanofibers of sugarcane bagasse. This study demonstrated that a very low-value agricultural waste product can be converted to a high performance nanocomposite (tensile strength: 140 MPa). The production process demonstrated in this study presents a cheap and fast method that involved downsizing (grinding) followed by a short partial dissolution time of 10 min. It was realized that by extending the duration of dissolution time there was better interfacial adhesion/welding between cellulose nanofiber and that generated a matrix phase that led to a good stress transfer capability in the nanocomposite. Since this ecocomposite is made completely of cellulose, it is fully biodegradable. Following this research, sugarcane bagasse can now be regarded as a promising low-cost raw material for high performance composite. Based on this study, it is also predictable that ACNC has potential for the development of barrier and protective film in food packaging industries. The tensile properties of ACNC film are at least comparable to better than those of other biodegradable or non-biodegradable film.

Acknowledgements

The authors gratefully acknowledge the financial support from the University of Tehran and Industrial Parks Co. of Alborz Province. The cooperation of Nano Novin Polymer Co. in the production of cellulose nanofibers using the disk grinder is also greatly acknowledged.

References

Abraham, E., Deepa, B., Pothan, L. A., Jacob, M., Thomas, S., Cvelbar, U., et al. (2011). Extraction of nanocellulose fibrils from lignocellulosic fibres: A novel approach. *Carbohydrate Polymers*, 1468–1475.

Afra, E., Yousefi, H., Hadilam, M. M., & Nishino, T. (2013). Comparative effect of mechanical beating and nanofibrillation of cellulose on paper properties made from bagasse and softwood pulps. *Carbohydrate Polymers*, *97*, 725–730.

Alila, S., Besbes, I., Rei Vilar, M., Mutjé, P., & Boufi, S. (2012). Non-woody plants as raw materials for production of microfibrillated cellulose (MFC): A comparative study. *Industrial Crops and Products*, *41*, 250–259.

Cerqueira, D. A., & Meireles, C. d. S. (2007). Optimization of sugarcane bagasse cellulose acetylation. *Carbohydrate Polymers*, *69*(3), 579–582.

Chandel, A. K., da Silva, S. S., Carvalho, W., & Singh, O. V. (2012). Sugarcane bagasse and leaves: Foreseeable biomass of biofuel and bio-products. *Journal of Chemical Technology and Biotechnology*, *87*, 11–20.

Chen, W., Yu, H., Liu, Y., Chen, P., Zhang, M., & Hai, Y. (2011). Individualization of cellulose nanofibers from wood using high-intensity ultrasonication combined with chemical pretreatments. *Carbohydrate Polymers*, *83*, 1804–1811.

Duchemin, B. J., Mathew, A. P., & Oksman, K. (2009). All-cellulose composites by partial dissolution in the ionic liquid 1-butyl-3-methylimidazolium chloride. *Composites Part A: Applied Science and Manufacturing*, *40*, 2031–2037.

Gibson, P. W., Lee, C., Ko, F., & Reneker, D. (2007). Application of nanofiber technology to nonwoven thermal insulation. *Journal of Engineered Fibers and Fabrics*, *2*, 32–40.

Gindl, W., & Keckes, J. (2005). All-cellulose nanocomposite. *Polymer*, *46*, 10221–10225.

Han, D., & Yan, L. (2010). Preparation of all-cellulose composite by selective dissolving of cellulose surface in PEG/NaOH aqueous solution. *Carbohydrate Polymers*, *79*, 614–619.

Huber, T., Müssig, J., Curnow, O., Pang, S., Bickerton, S., & Staiger, M. P. (2012). A critical review of all-cellulose composites. *Journal of Materials Science*, *47*, 1171–1186.

Jiménez, A., Fabra, M. J., Talens, P., & Chiralt, A. (2012). Effect of re-crystallization on tensile, optical and water vapour barrier properties of corn starch films containing fatty acids. *Food Hydrocolloids*, *26*, 302–310.

Kakudo, M., & Kasai, N. (1972). *X-ray Diffraction by Polymers*. Tokyo: Kodansha.

Kimura, S., Laosinchai, W., Itoh, T., Cui, X., Linder, C. R., & Brown, R. M. (1999). Immunogold labeling of rosette terminal cellulose-synthesizing complexes in the vascular plant *Vigna angularis*. *The Plant Cell Online*, *11*, 2075–2085.

Leitner, J., Hinterstoisser, B., Wastyn, M., Keckes, J., & Gindl, W. (2007). Sugar beet cellulose nanofibril-reinforced composites. *Cellulose*, *14*(5), 419–425.

Mauer, L., Smith, D., & Labuza, T. (2000). Water vapor permeability, mechanical, and structural properties of edible β-casein films. *International Dairy Journal*, *10*, 353–358.

Mazalevska, O., Struszczyk, M. H., Chrzanowski, M., & Krucińska, I. (2011). Application of electrospinning for vascular graft performance–preliminary results. *Fibres & Textiles in Eastern Europe*, *87*, 46–52.

Nishino, T., Matsuda, I., & Hirao, K. (2004). All-cellulose composite. *Macromolecules*, *37*, 7683–7687.
Park, H. J., & Chinnan, M. S. (1995). Gas and water vapor barrier properties of edible films from protein and cellulosic materials. *Journal of Food Engineering*, *25*(4), 497–507.
Park, H. M., Misra, M., Drzal, L. T., & Mohanty, A. K. (2004). "Green" nanocomposites from cellulose acetate bioplastic and clay: Effect of eco-friendly triethyl citrate plasticizer. *Biomacromolecules*, *5*(6), 2281–2288.
Piermaria, J. A., Pinotti, A., Garcia, M. A., & Abraham, A. G. (2009). Films based on kefiran, an exopolysaccharide obtained from kefir grain: Development and characterization. *Food Hydrocolloids*, *23*, 684–690.
Ray, S. S., & Bousmina, M. (2005). Biodegradable polymers and their silicate nanocomposites: In greening the 21st century materials world. *Progress in Materials Science*, *50*, 962–1079.
Rhim, J. W. (2011). Effect of clay contents on mechanical and water vapor barrier properties of agar-based nanocomposite films. *Carbohydrate Polymers*, *86*(2), 691–699.
Segal, L., Creely, J., Martin, A., & Conrad, C. (1959). An empirical method for estimating the degree of crystallinity of native cellulose using the X-ray diffractometer. *Textile Research Journal*, *29*, 786–794.
Shchipunov, Y. (2012). Bionanocomposites: Green sustainable materials for the near future. *Pure and Applied Chemistry*, *84*, 2579–2607.
Shellhammer, T. H., & Krochta, J. M. (1997). Edible coating and film barriers. *Lipids–Industrial Applications and Technology*, 453–479.
Smith, S. A. (1986). Polyethylene, low density. In *The Wiley Encyclopedia of Packaging Technology*. Wiley.
Soykeabkaew, N., Arimoto, N., Nishino, T., & Peijs, T. (2008). All-cellulose composites by surface selective dissolution of aligned ligno-cellulosic fibres. *Composites Science and Technology*, *68*(10), 2201–2207.
Soykeabkaew, N., Sian, C., Gea, S., Nishino, T., & Peijs, T. (2009). All-cellulose nanocomposites by surface selective dissolution of bacterial cellulose. *Cellulose*, *16*, 435–444.
Sun, J., Sun, X., Zhao, H., & Sun, R. (2004). Isolation and characterization of cellulose from sugarcane bagasse. *Polymer Degradation and Stability*, *84*(2), 331–339.
Svagan, A. J., Azizi Samir, M. A., & Berglund, L. A. (2007). Biomimetic polysaccharide nanocomposites of high cellulose content and high toughness. *Biomacromolecules*, *8*(8), 2556–2563.
Swatloski, R. P., Spear, S. K., Holbrey, J. D., & Rogers, R. D. (2002). Dissolution of cellulose with ionic liquids. *Journal of the American Chemical Society*, *124*, 4974–4975.
Tang, X., Kumar, P., Alavi, S., & Sandeep, K. (2012). Recent advances in biopolymers and biopolymer-based nanocomposites for food packaging materials. *Critical Reviews in Food Science and Nutrition*, *52*, 426–442.
Villar, J. C., Revilla Gómez, N., Carbajo, J. M., & Simón, J. L. (2009). Improving the use of kenaf for kraft pulping by using mixtures of bast and core fibres. *Industrial Crops and Products*, *29*, 301–307.
Yousefi, H., Nishino, T., Faezipour, M., Ebrahimi, G., Shakeri, A., & Morimune, S. (2010). All-cellulose nanocomposite made from nanofibrillated cellulose. *Advanced Composites Letters*, *19*, 204–209.
Yousefi, H., Faezipour, M., Nishino, T., Shakeri, A., & Ebrahimi, G. (2011). All-cellulose composite and nanocomposite made from partially dissolved micro-and nanofibers of canola straw. *Polymer Journal*, *43*, 559–564.
Yousefi, H., Nishino, T., Faezipour, M., Ebrahimi, G., & Shakeri, A. (2011). Direct fabrication of nanocomposite from cellulose microfibers using ionic liquid-based nanowelding. *Biomacromolecules*, *12*, 4080–4085.
Zimmermann, T., Bordeanu, N., & Strub, E. (2010). Properties of nanofibrillated cellulose from different raw materials and its reinforcement potential. *Carbohydrate Polymers*, *79*(4), 1086–1093.